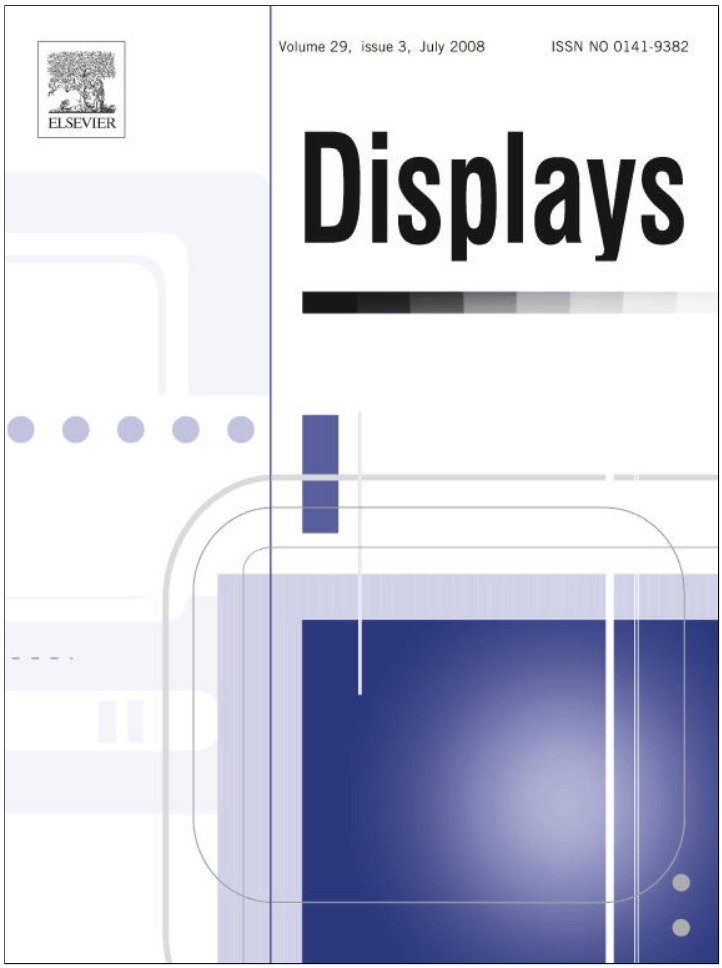

Available online at www.sciencedirect.com
ScienceDirect
Displays 29 (2008) 268–272
DISPLAYS
www.elsevier.com/locate/displa

Turn-on voltage reduction of organic light-emitting diode using a nickel-doped indium tin oxide anode prepared by single target sputtering

Ching-Ming Hsu *, Wen-Tuan Wu, Hsin-Hui Lee

Department of Electro-Optical Engineering, Southern Taiwan University, 1 Nan-Tai Street, Yung-Kang City, Tainan County 710, Taiwan

Received 6 August 2007; accepted 15 August 2007
Available online 21 August 2007

Abstract

Organic light-emitting diodes (OLEDs) with a nickel (Ni)-doped indium tin oxide (ITO) anode were fabricated. The Ni-doped ITO anode was prepared using sputter deposition of Ni–ITO single targets consisting of 1, 3 and 5 wt% of nickel. Turn-on voltage of OLED devices with the Ni-doped ITO anode was reduced by 2.5, 4 and 3.8 V for 1, 3 and 5 wt% targets, respectively. Half-luminance lifetime was improved by 2.5 times with a Ni(3 wt%)-ITO single target. The successful development in preparing Ni-doped ITO films by Ni–ITO single target sputtering allows this approach to be adopted for OLED manufacturing.

Keywords: Indium tin oxide (ITO); Organic light-emitting diode (OLED); Nickel (Ni)

1. Introduction

Indium tin oxide (ITO) is a well known transparent degenerate n-type semiconductor that is commonly used as an anode material for organic light-emitting diodes (OLEDs). For this application, ITO requires high surface work function and smooth surfaces in addition to high transparency and conductivity. Adjusting surface chemical states of an ITO anode by gaseous plasma bombardment [1–3], immersion in solutions [4,5], forming self assembled monolayers [6–8], introducing a top metallic oxide [9–11] or metal elements into ITO matrix [12,13] has been proved to be able to raise ITO surface work function, while chemical mechanical polishing [14,15] or plasma bombardment [16,17] can lead to an improved surface morphology. Raising ITO surface work function enhances hole injection from ITO into organics due to the reduced potential barrier at the ITO/organics interfaces. This should generally result in the improvement in the optoelectrical characteristics of OLED devices. Smoothing ITO surface topography on the other hand minimizes the occurrence of local high current flow and hence diminishes joule heat caused lifetime degradation.

Until now, gaseous plasma surface treatment of ITO has been the major approach to raise ITO surface work function in the industrial manufacturing of OLEDs, whereas surface smoothing is generally conducted by the process control of ITO deposition or post-surface polishing. However, our recent studies which add high work function nickel (Ni) atoms into ITO matrix have shown their high potential in improving overall OLED performances [18]. This is because Ni is a high work function material ($\Phi \sim 5.0$ eV) and can form NiO_x phases when introduced into ITO matrix. The existence of NiO_x phase can raise ITO work function to a level of 5.4 eV which is much higher than that of the gaseous plasma treated ITO ($\Phi \sim 4.6$ eV). Hence, a large reduction in the operation voltage of OLED devices with a Ni–ITO/organics interface is usually observed. Our previous work has demonstrated that the turn-on voltage can be reduced by 2.3 V for a

* Corresponding author.
E-mail address: tedhsu@mail.stut.edu.tw (C.-M. Hsu).

0141-9382/$ - see front matter © 2007 Elsevier B.V. All rights reserved.
doi:10.1016/j.displa.2007.08.009

OLED device with an Ni(1.8 wt%)-doped ITO anode. Especially noticed is that the incorporation of Ni in the ITO matrix also yields a smoother ITO surface, leading to the enhanced device lifetime [19,20].

Yet, the preparation of the Ni-doped ITO anode was conducted by a Ni–ITO co-sputter method that is difficult to be implemented into an in-line mass production system. In this article, we report on the formation of Ni-doped ITO film using a Ni–ITO single target with various Ni concentrations. The effects of the Ni-doped ITO anode prepared with this single target approach on the characteristics of OLED devices are investigated, and the results are compared with those fabricated with the Ni–ITO co-sputter method. The use of Ni–ITO single target allows the synthesis of Ni-doped ITO film be directly adopted in the current production line.

2. Device fabrication

OLED devices with a structure of Al/tris(8-hydroxyquinoline) aluminum (Alq3)/*N*,*N*′-bis-(1-naphthyl)-*N*,*N*′-diphenyl-1,1′biphenyl-4,4′-diamine(NPB)/ nickel-doped ITO/PET film were employed as an test vehicle. Fabrication of the device began with the deposition of a 100 nm undoped ITO film on a PET substrate using d.c. sputtering at substrate temperature of 100 °C. A 50 nm Ni-doped ITO film was then immediately deposited in the same sputter chamber with a Ni–ITO single target using an r.f. power of 30 W. The schematic of the sputter apparatus is shown in Fig. 1. The Ni–ITO single target consists of 1, 3 and 5 wt% of Ni and was placed around 10 cm below the substrate holder which was rotated at a speed of 15 r.p.m. to ensure a uniform distribution of ITO film thickness and Ni concentration. The Ni-doped ITO/ITO films were patterned by a standard photolithography process to form a proper shape for serving as an anode for the device.

The Ni-doped ITO films were then loaded into a cluster system where O_2 plasma treatment was conducted before moving to a resistive thermal evaporator for depositing NPB and Alq_3 layers. The NPB and Alq_3 films were sequentially deposited with the same deposition rate of 0.1 Å/s and without the substrate being heated. After the deposition of the organic layers, the substrates were transferred into an e-beam evaporator without breaking the vacuum for the deposition of LiF buffer layer and Al cathode. A metallic shadow mask was used to define the shape of counterpart electrode to the ITO anode. During the depositions, the substrate temperature was recorded below 30 °C. The complete OLED devices, having a double heterojunction structure of Al(100 nm)/LiF(0.05 nm)/Alq_3(35 nm) NPB(20 nm)/Ni-doped ITO(50 nm)/undoped ITO(100 nm), were immediately characterized using an HP4155B *I-V* meter for the current–voltage (*I–V*) measurement and a Photosearch PR650 C.I.E. spectrometer for the luminance measurement. For comparison, device with an undoped ITO anode of 150 nm was also fabricated.

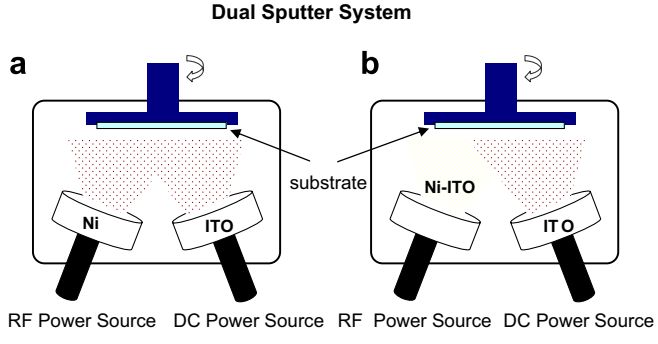

Fig. 1. Schematic of sputter apparatus used for depositing Ni-doped ITO films, (a) co-sputter process, (b) single target sputter process.

3. Results and discussions

To investigate the effects of Ni-doped ITO films on the performance of OLED devices, the stacked Ni-doped ITO/ITO films were characterized with a four-point probe and a Hitachi 3310 UV spectrometer for sheet resistance and optical transmittance, respectively. The in-depth Ni atomic concentration was analyzed using an Auger Electron Spectrometer (AES; VG MicroLab 310-F), and the surface morphology was measured by an atomic force microscope. The average Ni concentration calculated from AES depth profiling is 1.0, 2.0 and 2.7 wt% for the Ni–ITO target with the nominal Ni concentration of 1, 3, and 5%, respectively. This correspondingly yields a sticking coefficient of Ni of 1, 0.67 and 0.54, suggesting that the percentage of Ni atoms out of the single target is less incorporated in the ITO matrix as the Ni concentration in Ni–ITO target increases. The phenomenon is similar to what has been observed in the Ni–ITO co-sputter scheme in which Ni target sputtered with 10, 30 and 50 W r.f. power generates 1.1, 1.8 and 2.6 wt% of Ni in the ITO matrix. The corresponding coefficient is 1.1, 0.6 and 0.52.

Fig. 2 shows the sheet resistance and optical transmittance of the stacked Ni-doped ITO/ITO film as a function of the nominal Ni concentration. It can be seen that the stacked films have much higher sheet resistance (>109 ohm/sq) than the undoped ITO film (~79 ohm/sq), whereas their optical transmittances (87.1–91.2%) are similar to the undoped ITO film (88.8%). These results are inconsistent with those obtained by co-sputtering method [19], in which both sheet resistance and optical transmittance decrease with the increasing Ni concentration. This implies that in the co-sputter system Ni atoms departing from the r.f. sputter source would mostly exist interstitially in the ITO lattice. Individual Ni atoms provide extra free electrons that increase film conductivity but degrade the optical density due to the increased electron shielding effect to the photons. In this single target system, the way Ni atoms appeared in the ITO matrix should be more complicated. Ni atoms might replace the lattice site of Sn, exist interstitially in the ITO lattice, or react with oxygen to form NiO_x phases. Since the introduction of Ni atoms does

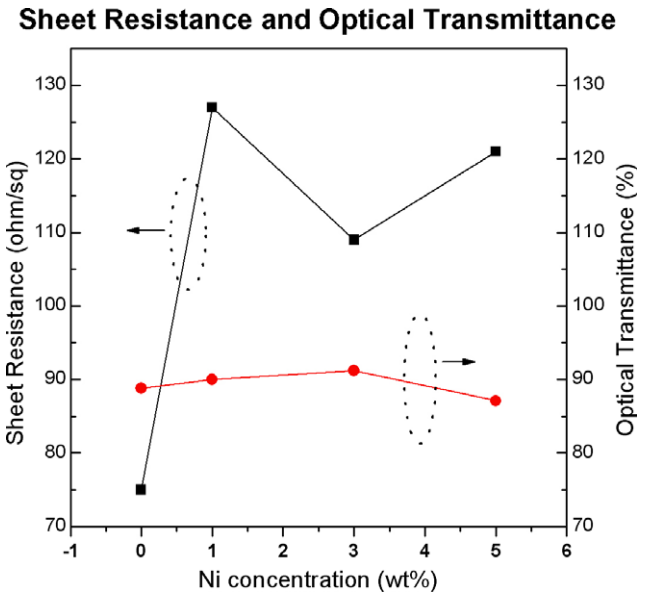

Fig. 2. Sheet resistance and optical transmittance of the Ni-doped ITO/ITO film as a function of the nominal Ni concentration in the Ni–ITO single target.

not increase the film conductivity, the dominating phase may be NiO_x that provides no extra carriers and is transparent. Fig. 3 reveals the existence of the NiO_x phase using a Fourier Transform Infrared Spectrometer (FTIR). The variation at wavenumber of $\sim$3000 cm^{-1} represents the N–O absorption, and the level of variation increases with the Ni concentration.

Comparing only the stacked Ni-doped ITO/ITO films, one can find that the film deposited with the 3% Ni–ITO target has the lowest sheet resistance and the highest optical transmittance. Generally, as the amount of Ni atoms increases the carrier concentration would increase by precipitating in the ITO matrix. However, the formation of the NiO_x in the ITO matrix would limit such a process, and hence the carrier concentration might not increase with the increasing Ni atoms. This was verified by the Hall-effect measurement from which the carrier concentration was 1.6 and $0.7 \times 10^{20}/cm^3$ for the target with Ni = 1 and 3 wt%, respectively. If Ni replaces the lattice side of Sn, the Ni^{+2} would increase the amount of hole carrier but decrease the electron carriers (from the loss in Sn^{+4}) at the same rate. In such a case the film sheet resistance would increase because of the decrease in carrier mobility. On the other hand, the formation of NiO_x may consume oxygen atoms and generate more oxygen vacancies in the ITO structure. Such a process would increase the carrier concentration through the oxygen vacancy mechanism and at the same time degrade the carrier mobility by the impurity scattering mechanism. From the discussions above, the tendency in electrical and optical properties of the Ni-doped ITO film is not predictable with the Ni–ITO single target approach, and this should be resulted from the complicated development of the state of Ni atoms in the course of ITO sputter deposition.

Fig. 4 shows the *I–V* characteristics of the OLED devices. It is clear the *I–V* characteristics were improved when the devices had a Ni-doped ITO anode. The threshold voltage determined at 0.1 A/m^2 was 3.56, 3.46 and 4.26 V for 1, 2 and 2.7 wt% Ni-doped devices, which was up to 1.52 V lower than that of undoped one (4.98 V). Our previous work with a Ni–ITO co-sputter method [18] showed that OLED devices with an Ni(1.8 wt%) and Ni(2.6 wt%)-doped ITO anode had similar *I–V* characteristics. Their threshold voltages could be reduced up to 3.2 V compared with the undoped device. Whereas In this study, the device with a Ni(2 wt%)-doped ITO anode had the best *I–V* characteristic but with a Ni(2.7 wt%)-doped ITO anode had the worst. Comparing the results of *I–V* characteristics between these two approaches, we can presume (1) the actual Ni concentration over 2 wt% with this single target scheme degrades the device performance, whereas it does so for that over 2.6 wt% with a co-sputter method; (2) Ni or NiO_x phases should be more abundant at the

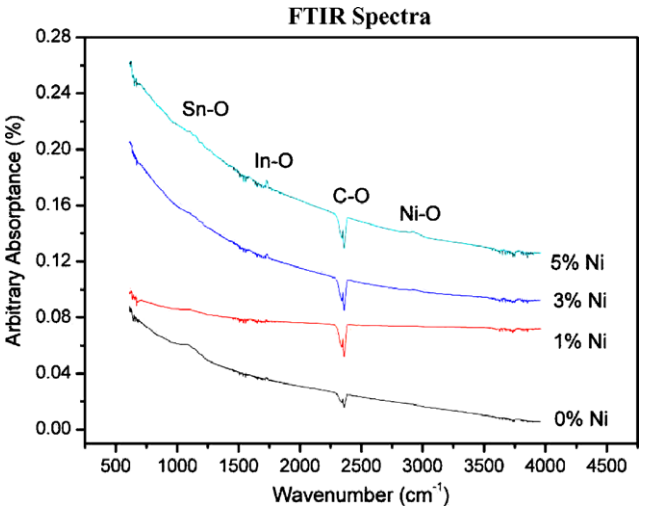

Fig. 3. FTIR spectra of the Ni-doped and undoped ITO films.

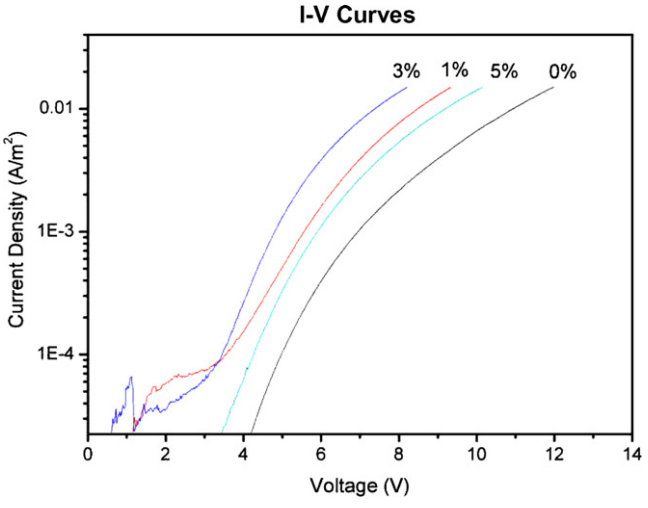

Fig. 4. *I–V* characteristics of OLED devices with and without a Ni-doped ITO anode.

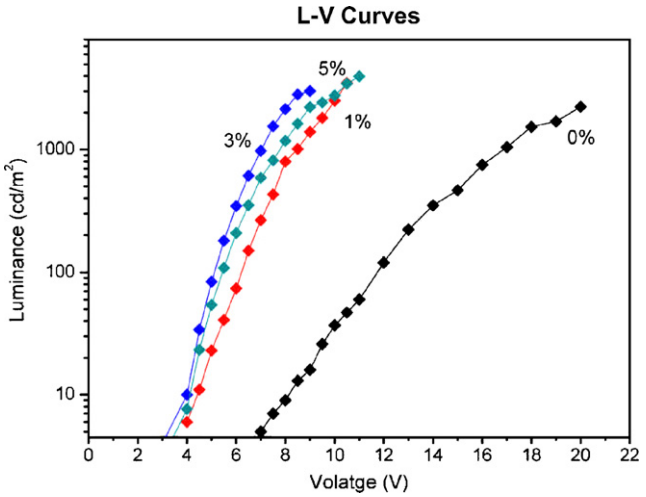

Fig. 5. L–V characteristics of OLED devices with and without a Ni-doped ITO anode.

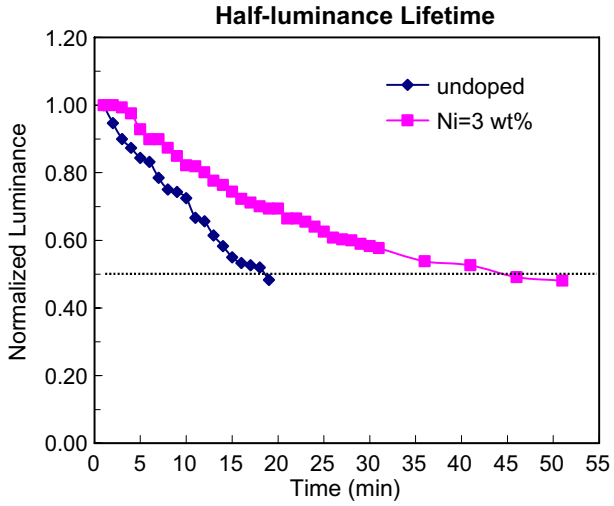

Fig. 6. Half-luminance lifetime spectra of the Ni(3 wt%)-doped and undoped OLED devices.

ITO/NPB interfaces with the co-sputter method, because its reduction in the threshold voltage was more efficient.

The L–V characteristics of the OLED devices are presented in Fig. 5. Similar to the I–V characteristic, the L–V characteristics were improved when the devices was inserted with a Ni-doped ITO anode. The best I–V characteristic was for the device with the Ni(2 wt%)-doped ITO anode. The turn-on voltages, determined at 10 cd/m^2, are 4.5, 4.0 and 4.1 V for the 1, 2 and 2.7 wt% Ni-doped ITO device, respectively, reduced by around 4 V compared with the un-doped device ($V_{on} = 8.1$ V). The drop in the turn-on voltage is believed due to the elevated ITO surface work function, attributed to the appearance of Ni atoms or NiO_x phases at the ITO/NPB interface as discussed elsewhere [19]. The L–V characteristic of the 2.7 wt% Ni-doped ITO device was also found inferior to the 2 wt% one. The reason may be the slight drop in optical transmittance and higher sheet resistance for the 2.7 wt% Ni-doped ITO film.

Fig. 6 demonstrates the results of the half-luminance lifetime test for the Ni(2 wt%)-doped and undoped devices. The devices were driven to have an initial luminance of 600 cd/m^2, and all the following measured luminance with time were normalized to this value. It can be seen from the spectra that the OLED device with the Ni(2 wt%)-doped ITO anode had a half-luminance lifetime of 45 min, around 2.5 times that of the undoped device (18.5 min). This is about the same result as reported in our previous work with a co-sputter method [20]. Smoother surface roughness that caused better ITO/NPB contact and less local joule heating was believed to be the main factor for the improved lifetime. In this study, the AFM surface roughness was 0.54 nm and 0.85 nm for the Ni(2 wt%)-doped and undoped ITO anodes, respectively. The fact that the incorporation of Ni atoms during ITO sputter deposition could reduce the surface roughness of an ITO film is the same with a single target approach as with a co-sputter method.

As mentioned earlier, fabricating a Ni-doped ITO film by a Ni–ITO co-sputter scheme is difficult to be adopted in an existing mass production line. Hence the successful development of OLED devices with a Ni-doped ITO anode using the Ni–ITO single target approach in this study is important and would allow the Ni-doped ITO process be integrated into the mass production line.

4. Conclusions

This article demonstrated that OLED devices with a Ni-doped ITO anode fabricated using a Ni–ITO single target performed better characteristics than that without Ni-doped one. A threshold voltage drop up to 1.52 V and a turn-on voltage reduction by 4 V have been achieved for the device with an anode sputtered with a Ni(3 wt%)-ITO single target. The half-luminance lifetime was enhanced by 2.5 times, attributed to the improved characteristics and surface roughness. The characteristics of OLED devices were found comparable to those synthesized using a co-sputter method. The use of Ni–ITO single target sputtering instead of co-sputtering for fabricating Ni-doped ITO anodes is more feasible for this scheme to be adopted for industrial manufacturing of OLEDs.

Acknowledgements

The authors would like to thank the National Science Council of Taiwan for financially supporting this work under Contract No. NSC-95-2221-E-218-047. Thanks also go to Center for Advanced Optoelectronics of National Cheng Kung University for partially funding this project and providing analytical instruments.

References

[1] C. C Wu, C.I. Wu, J.C. Sturm, A. Kahn, Appl. Phys. Lett. 70 (1997) 1348.
[2] B. Choi, H. Yoon, H.H. Lee, Appl. Phys. Lett. 76 (2000) 412.
[3] C.T. Lee, B.T. Tang, H.Y. Lee, Thin Solid Films 386 (1) (2001) 105.

[4] F. Li, H. Tang, J. Shinar, O. Resto, S.Z. Weise, Appl. Phys. Lett. 70 (1997) 2741.
[5] Z.Z. You, J.Y. Dong, Microelectron. J. 38 (2007) 108.
[6] S.K. So, W.K. Choi, C.H. Cheng, L.M. Leung, C.F. Kwong, Appl. Phys. A Mater. Sci. Process. 68 (1999) 447.
[7] J. Schwartz, E.L. Bruner, N. Koch, A.R. Span, S.L. Bernasek, A. Kahn, Synth. Met. 138 (2003) 223.
[8] X.H. Sun, L.F. Cheng, M.W. Liu, L.S. Liao, N.B. Wong, C.S. Lee, S.T. Lee, Chem. Phys. Lett. 370 (2003) 425.
[9] I.D. Parker, J. Appl. Phys. 75 (1994) 1656.
[10] P.W.M. Blom, M.J.M. de Jong, J.J.M. Vleggaar, Appl. Phys. Let. 68 (1996) 3308.
[11] I.M. Chan, T.Y. Hsu, F.C. Hong, Appl. Phys. Let. 81 (2002) 1899.
[12] T.J. Marks, J.G.C. Veinot, J. Cui, H. Yan, A. Wang, N.L. Edleman, J. Ni, Q. Huang, P. Lee, N.R. Armstrong, Synth. Met. 127 (2002) 29.
[13] A.J. Freeman, K.R. Poeppelemier, T.D. Mason, R.P.H. Chang, T.J. Marks, MRS Bull. 25 (2000) 45.
[14] M. Matsumura, Y. Jinde, Synth. Met. 91 (1997) 197.
[15] J.-S. Lim, P.-K. Shin, Appl. Surf. Sci. 253 (2007) 2828.
[16] S. Jung, N.G. Park, M.Y. Kwak, B.O. Kim, K.H. Choi, Y.J. Cho, Y.K. Kim, Y.S. Kim, Optic. Mater. 21 (2002) 235.
[17] S.M. Joeng, W.H. Koo, S.H. Choi, S.J. Jo, H.K. Baik, S. J Lee, K.M. Song, Thin Solid Films 475 (2005) 227.
[18] C.M. Hsu, W.T. Wu, Appl. Phys. Lett. 85 (2004) 840.
[19] C.M. Hsu, J.W. Lee, T.H. Meen, W.T. Wu, Thin Solid Films 474 (2005) 19.
[20] C.M. Hsu, W.C. Hsu, C.S. Kuo, W.T. Wu, in: Proceedings of International Display Workshop, Takamatsu, Japan, 2005, p. 683.